PROCEEDINGS OF SPIE

SPIEDigitalLibrary.org/conference-proceedings-of-spie

Embedded system upgrade based on Raspberry Pi computer for a 23/31 GHz dual-channel water vapor radiometer

Ferrusca , Daniel, Cuazoson, Jetzael, Contreras, Jesús, Hiriart, David, Ibarra , Eduardo, et al.

Daniel Ferrusca , Jetzael Cuazoson, Jesús Contreras, David Hiriart, Eduardo Ibarra , Stanley Kurtz, Tinus Stander, Miguel Velázquez, "Embedded system upgrade based on Raspberry Pi computer for a 23/31 GHz dual-channel water vapor radiometer," Proc. SPIE 11445, Ground-based and Airborne Telescopes VIII, 1144586 (13 December 2020); doi: 10.1117/12.2561733

SPIE.

Event: SPIE Astronomical Telescopes + Instrumentation, 2020, Online Only

Embedded system upgrade based on Raspberry Pi computer for a 23/31 GHz dual-channel water vapor radiometer

Daniel Ferrusca[*a], Jetzael Cuazoson[b]. Jesús Contreras[a], David Hiriart[d], Eduardo Ibarra[c], Stanley Kurtz[c], Tinus Stander[e], Miguel Velázquez[a]

[a]Instituto Nacional de Astrofísica, Óptica y Electrónica, Luis Enrique Erro #1, Tonantzintla, PUE, México;
[b]Universidad Juárez Autónoma de Tabasco, Carr. Cunduacán-Jalpa KM 1, Cunduacán, TAB, México;
[c]Instituto de Radiastronomía y Astrofísica UNAM, Antigua Carretera a Pátcuaro #8701, Morelia, MIC, México;
[d]Instituto de Astronomía Campus Ensenada UNAM, Carr. Tijuana-Ensenada KM 107, Ensenada, BCN, México;
[e]University of Pretoria, University Road, Pretoria, South Africa

ABSTRACT

We present the refurbishment of a 23.8/31.5 GHz tipping radiometer (WVR-III) to characterize atmospheric opacity for astronomical sites. The mid-life upgrade will bring new life to the 20-year-old WVR-III with most control functions now embedded on a Raspberry PI 3B+ (RPi-3B+). The radiometer will be installed alongside the 225 GHz radiometer at the *Large Millimeter Telescope* site in Mexico and in 2021 it will be taken to the *Hartebeesthoek Radio Astronomy Observatory* in South Africa. Later, it will be deployed to *Mt Gamsberg, Namibia* to perform PWV site surveying for potential future radio astronomy telescopes. This paper describes the new control and data acquisition sub-systems that are controlled by the RPi-3B+.

Keywords: Opacity, radiometer, PWV, Raspberry, embedded system, Large Millimeter Telescope

1. INTRODUCTION

Earth's atmosphere is made up of several chemical elements, compounds and material that influence visibility into outer space at certain wavelengths of electromagnetic spectrum. Radio astronomy is a science that considers atmospheric visibility as a relevant and significant topic. Radio astronomy focuses on the study of far infrared, millimeter/submillimeter (and some shortwave radio) wavelengths, and precipitable water vapor (PWV) is known as the main absorption and scattering component in atmosphere for these frequencies, although other molecules (as oxygen, ozone, carbon dioxide) also have an influence [1]. However, the atmosphere also provides radiation windows for specific wavelengths where the scattering and absorption effects are lessened. One instrument that helps determine the amount of signal attenuation in these windows is known as radiometer [2].

The radiometer is made up of different electronic devices that perform the radiation readings captured by the instrument to obtain a constant voltage signal proportional to the noise power of the incoming signal. The radiometer consists of horn antennas, an electronic RF receiver, an acquisition system, and data logging system. According to the tipping method, the radiometers also have a servo-mechanical control system to move the antennas or mirrors, as well as a weather station to monitor local environment variables [3].

Figure 1, shows the WVR-III which is a dual-channel water vapor radiometer from the *Hartebeesthoek Radio Astronomy Observatory* (HartRAO) in South Africa. The instrument was used for several radio astronomy site testing and geodesy purposes in the past decade to the end of its useful life in 2007. The last activity of WVR-III was the *CONT05* campaign of *VLBI* carried out in September, 2005 at HartRAO [4].

[*] Email: *dferrus@inaoep.mx*, Phone: (+52) 222-266-3100, Ext. 1304

Ground-based and Airborne Telescopes VIII, edited by Heather K. Marshall, Jason Spyromilio, Tomonori Usuda, Proc. of SPIE Vol. 11445, 1144586 · © 2020 SPIE
CCC code: 0277-786X/20/$21 · doi: 10.1117/12.2561733

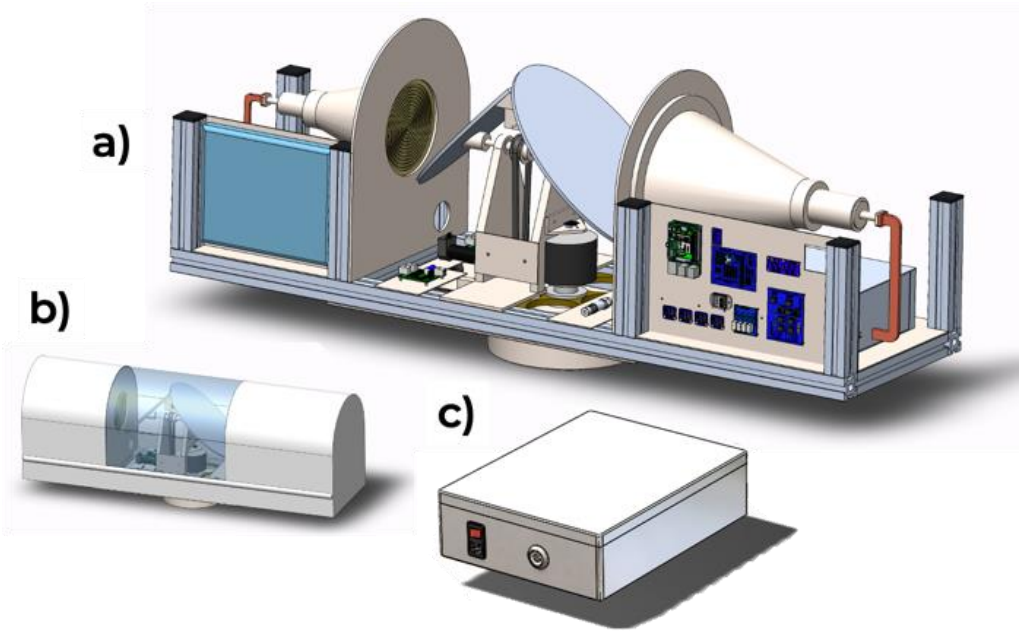

Figure 1. CAD Models of a) WVR-III radiometer (real size), b) radiometer's case (1:4 scaled) and c) main power supply (real size).

Currently, the *National Autonomous University of Mexico* (UNAM), the *National Institute of Astrophysics, Optics and Electronics* (INAOE) and the *University of Pretoria* (UP), under the program called "*Development of Technology, Data and Capacity in Millimeter Water Vapor Radiometry for Radio Astronomy*" [12] are developing new technologies for water vapor radiometry using new data reduction methods for opacity, planar antennas technologies, and single board computer digital back-ends architectures for radiometers. In that way, the refurbishment of WVR-III is one of the main tasks of the project to upgrade the instrument with new technologies that help to characterize new sites for future radio telescopes observatories.

Originally, the WVR-III was fully controlled by an external computer and a microcontroller which were responsible for data acquisition, data flow and control of the servo-mechanical system using serial communication interface with each component. The computer was integrated with a graphical user interface based in *LabVIEW* 6.0 [5]. Due to the lifetime of the components many of them started to fail, and the radiometer became inoperable. In order to extend the operating lifetime of the WVR-III, it was sent from UP to INAOE to upgrade the system. Faced with limited documentation, we had to do reverse-engineer of some parts of the system to determine how systems were interconnected with software tasks. In the next section we describe the INAOE´s team refurbishment plan based in new-generation technologies, involving an embedded system based in a single-board computer: the *Raspberry Pi 3 B+* and hardware attached on top (HATs) boards with new functionalities.

2. DESIGN OF EMBEDDED SYSTEM

The upgrade proposal of WVR-III consisted of the replacement of all electronics components and keeping both 23 and 31 GHz receivers, the chassis and mechanical components for azimuth and elevation. Using a new architecture for the radiometer, we were responsible for acquisition of electronic components, design, assembly and validation. In order to keep the RF receivers of WVR-III, we adapted the architecture of the system based in both *RPG-Tip-225* [6] and *Survey 3* [7], as these are the main radiometers of *Large Millimeter Telescope Alfonso Serrano* and *San Pedro Mártir National Astronomy Observatory* in Mexico, respectively. The new system is based in the diagram showed in Figure 2 with all its associated components to perform the tasks involved in water vapor radiometry.

2.1 Central Processing Unit

The *Raspberry Pi* (especially model 3 B+) is a low-cost and powerful Single-Board Computer with hardware interfaces and serial communication, useful for many applications. This is the main component of our system, and it controls

almost all processes of the radiometer including servo-mechanical control, RF signal acquisition and processing, switching in RF receivers, reading of weather station, data logging and data export.

The computer executes a *Python* code that contains every script for each board: RTD amplifiers; switches driver; temperature and humidity sensor; barometric pressure sensor; 9-DOF inertial measurement unit; PWM interface; analog to digital converter; 4G-LTE network interface. The functionality of each subsystem is described in the following sections.

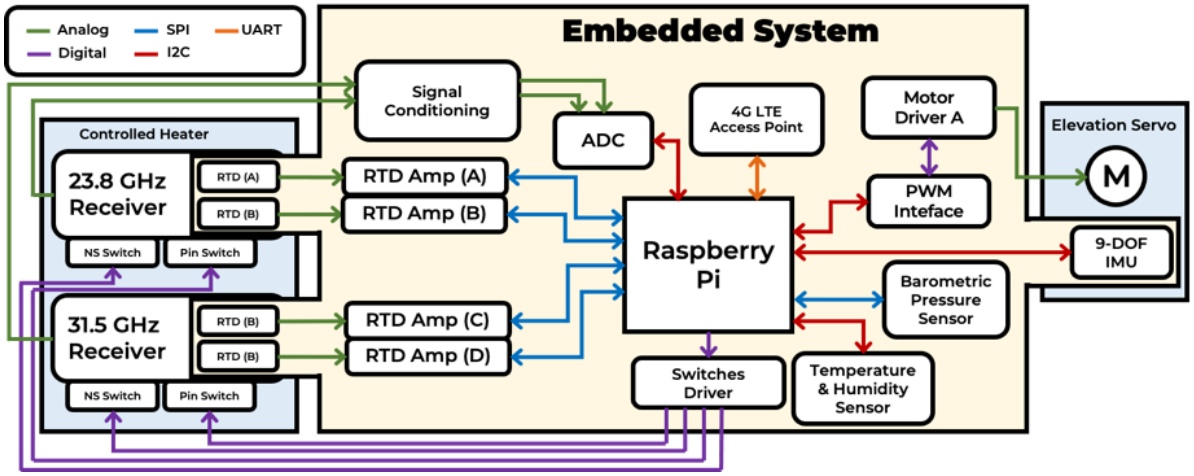

Figure 2. Block diagram of the new architecture for the WVR-III of the embedded system based on *Raspberry Pi* computer.

2.2 Control and readout in RF receivers

The RF receivers of WVR-III are total power radiometers with Dicke switches for calibration. They see three different temperature sources: sky, noise source and 50Ω reference load. The circuit given by [5] is reproduced in Figure 3; it has two input ports for switching the loads and the output port for the DC RF signal.

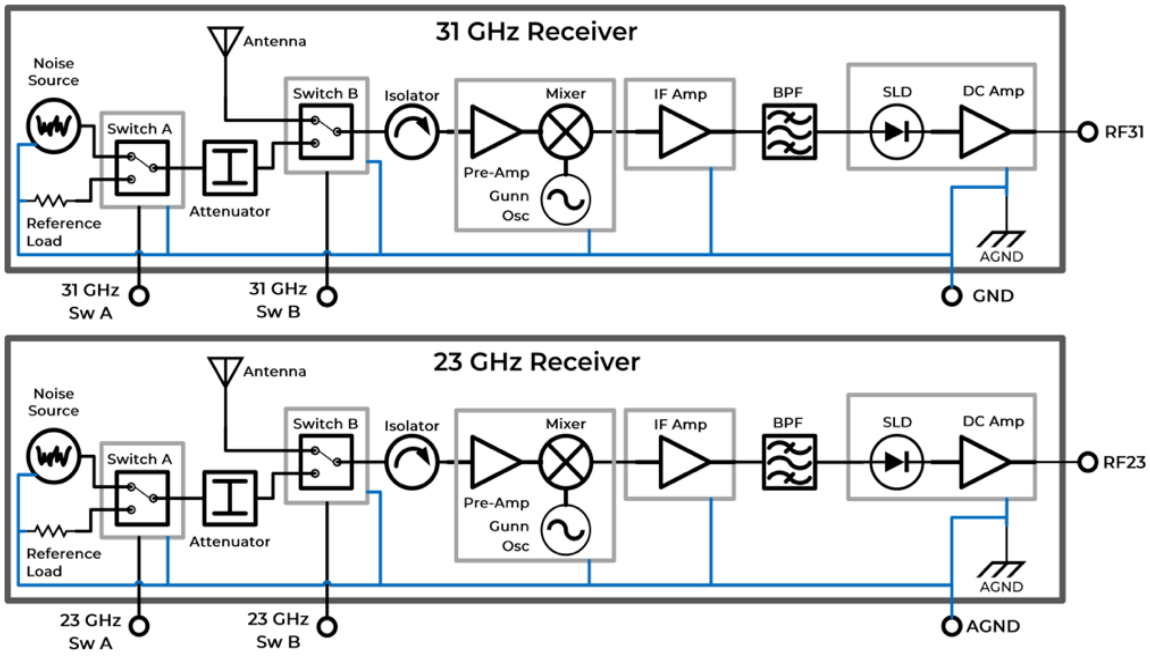

Figure 3. The RF receivers of WVR-III are based in the Dicke radiometer. Schematics of WVR-III's RF receivers.

2.2.1 RF thermal load switching

Each RF receiver of WVR-III has two switches:

- The "Noise Source Switch" controls the path of the signal from noise source. It is polarized with -10 V (ON) for both receivers and 0.75 V (OFF) for 31 GHz receiver and 2.75 V (OFF) for 23 GHz receiver. In OFF mode, the switch behaves like a 50Ω reference load. In that way, when the switch is ON, we see the Noise Source signal at output. When the switch is OFF, we see the signal of the reference load.
- The "Pin Switch" allows us to switch between the noise source/reference charge and the antenna. This switch has a TTL interface; it is polarized with 5 V signal. For 0 V (OFF), the switch sees the antenna's way. For 5 V, the switch sees the noise source's way.

In order to control these switches, we designed and implemented a galvanic-isolated interface (Switches Driver board, see Figure 4) based in V23079 relays of *Axicom* used for telecom, low power applications, medical and automation purposes. At the input, the interface has BJT transistors to drive the relays, and the transistors are driven with the *Raspberry Pi*'s GPIO. At the output, the supply and control nodes are connected to the switches.

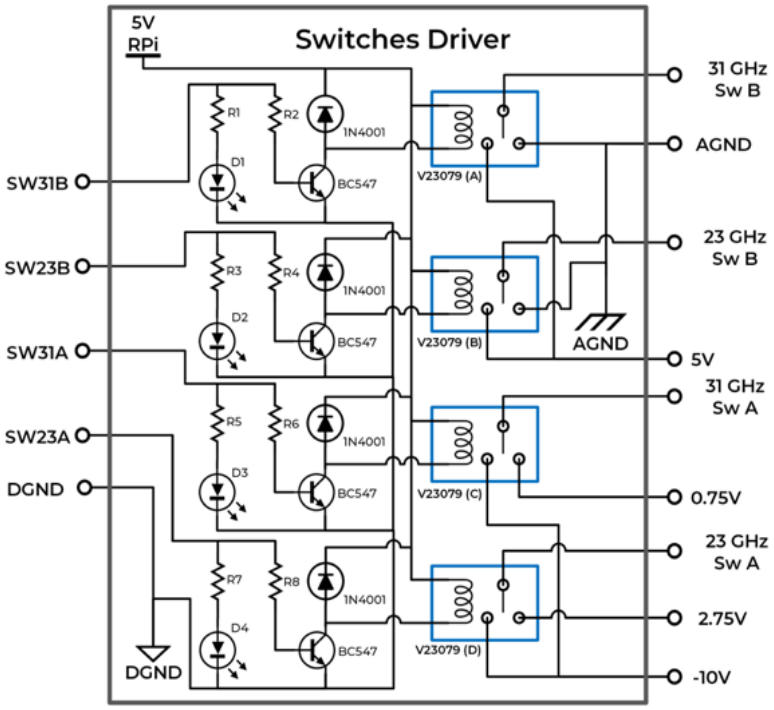

Figure 4. Schematics of Switches Driver circuit for RF receivers.

We implemented a *Python* script to control the states of the switches with the designed board. This routine is based on the manufacturer's original switching mode. The truth table and times of each scenario is showed in Table 1.

Table 1. Truth table of RF switches states.

Noise Source Switch (Sw A)	Pin Switch (Sw B)	Output Signal	Time Interval
OFF	OFF	Antenna	7.35 s
OFF	ON	50 Ω Load	4.0 s
ON	OFF	Antenna	-
ON	ON	Noise Source	3.95 s

2.2.2 ADC Conditioning

Since the RF receivers deliver a DC voltage proportional to noise power from incoming RF signal, we implement a signal conditioner based in Op-Amps for ADC readings. As the ADC has a reference voltage of 5 V, we reduce the RF signal of 0 – 10 V with the circuit shown in Figure 5. As circuit reads a constant voltage, we design a proportional amplification stage followed by linear opto-isolator in such a way that the output voltage V_o is the result of an amplification of the input voltage V_i as:

$$V_o = 0.40912\, V_i \approx 0.4 V_i \tag{1}$$

obtained analytically and verified experimentally.

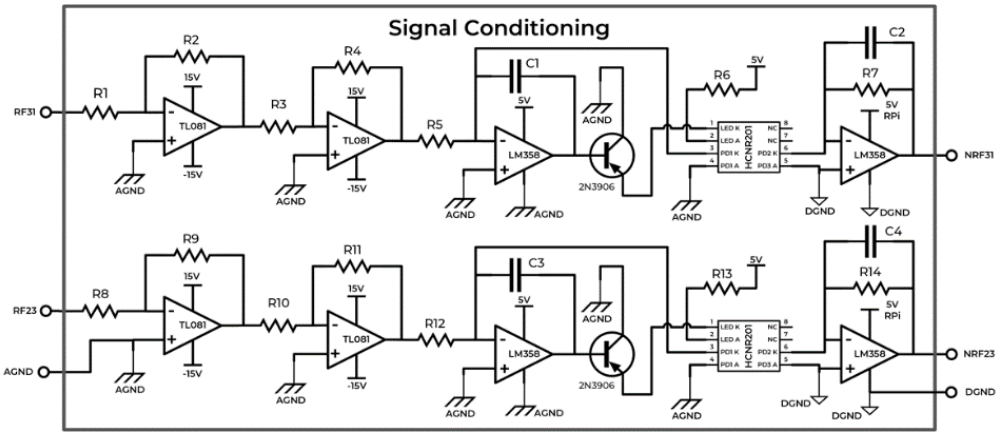

Figure 5. Signal conditioning circuit for ADC.

This circuit has and opto-isolated interface to keep analog supply voltages away from digital supply voltages. The main component of this circuit is a high-linearity analog optocoupler: the HCNR201 chip of *Avago Technologies*. The output is connected directly to *Adafruit*'s ADS1115 development board to acquire both 31 GHz and 23 GHz signal. A *Python* script registers the voltages digitized by ADS1115 of each receiver in a general data report file. The interconnection for the ADS1115 can be found elsewhere [13].

We did a Gain-Phase characterization of this circuit in order to compensate the gain loss via software. We used *Bode* plots (using a *Keysight* oscilloscope) to determine the linear regions of the signal and the real gains. After that, we set this value in respective *Python* script.

2.2.3 Receiver temperatures

The WVR-III provides an external temperature controller to keep RF receivers base plates thermally stable. This controller is GCS-23A-R/E made by *Shinko Techno* and it has several control modes, including PID. This device closed its loop using an RTD (Resistive Temperature Detector) sensor located at the edges of each receiver's plates to guarantee a certain temperature around the plates. Additionally, our system implements four modules for temperature monitoring inside each receiver by using 3-wire PT100 sensors coupled to *Adafruit*'s MAX31865 which allows internal RTD calibration and sends the data via SPI protocol to the *Raspberry Pi*. A *Python* script is used to communicate with these boards, acquiring each temperature and applying a post-acquisition median-filter using NUMPY library by *NumPy Project* [8].

2.3 Servo-mechanism control

Originally, the WVR-III was design to move in azimuth and elevation. Since the radiometer is going to be installed alongside other radiometers for initial characterization, we consider only the movement of the elevation mirrors used to generate tip curves.

The elevation mechanism is controlled by using *Adafruit*'s PCA9685 serial PWM interface followed by *DFRobot* AQMH2407 dual H bridge to drive the servo. Applying digital data from the *Raspberry Pi*, we acquired the output

angle of the mechanism in open-loop mode with *Adafruit*'s LSM9DS1 9-DOF inertial measurement unit [14]. After using *MATLAB*'s *Curve Fitting Tool* [9] and *System Identification* [10], we obtained the general model of the servomechanism as:

$$G(s) = \frac{\theta_e}{V_e} = \frac{0.4888s + 0.1543}{s^2 + 0.08397s + 1.183 \times 10^{-16}} \quad (2)$$

Finally, we used *MATLAB*'s *PID Tuner* [11] using the above equation to get the parameters of the PI controller, the representative block diagram of which is shown in Figure 6.

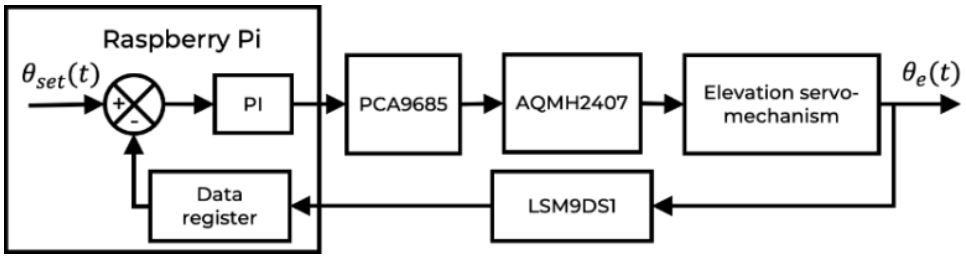

Figure 6. Closed-loop block diagram with controller of elevation servo-mechanism and electronic interfaces.

2.4 Weather station

The radiometer´s weather station is a complementary module for astronomers but also useful in the data reduction method used. Our weather station includes: a temperature and humidity sensor based on the *Adafruit*'s HTU21 board with *Python* script implementation which uses the I2C interface to communicate with the *Raspberry Pi* as well as a barometric pressure sensor based on the *Adafruit*'s BMP280 board which is a piezo-resistive sensor and communicates via the SPI interface [15,16].

2.5 Communication modules

The new WVR-III includes ethernet, 4G-LTE and Wi-Fi capabilities to communicate with external computers through *Raspbian* operating system, and allows to upload the collected data to internet file hosting services such as *Google Drive* for storage and online query. The devices used for these purposes are the: EC25 as network provider, made by *Quectel* [17] and 3G/4G Base Shield as USB network interface made by *SixFab* [18]. The EC25 is mounted over the Base Shield, which is connected via USB port directly to the Raspberry Pi.

3. RESULTS

The subsystems described in previous sections were interconnected to the *Raspberry Pi* by using the different serial interfaces as SPI, I2C, UART and USB according to Figure 2, and *Python* scripts were developed to call the libraries of modules, set RF switches states, acquire RF signals, readout casing temperatures and weather variables, and define mirrors positions (air masses) and integration time.

The data register stores all the collected data in a text file. This file has a singular column format based on the original WVR-III's data file [5]. Each row has the following sequence by columns: **DATE TIME** (MM/DD/YYYY hh:mm:ss format), **AIRMASS** (elevation angle in degrees), **REAL_POS** (reached elevation angle), **TA31** (31 GHz Rx. Plate temp.), **TN31** (31 GHz Rx noise source temp.), **TA23** (23 GHz Rx. Plate temp.), **TN23** (23 GHz Rx. Noise source temp.), **VRF31_MIRROR** (mirror data of 31 GHz Rx.), **VRF23_MIRROR** (mirror data of 23 GHz Rx.), **VRF31_50R** (50 Ω reference load temp. of 31 GHz Rx.), **VRF23_50R** (50 Ω reference load temp. of 23 GHz Rx.), **VRF31_NS** (Noise source temp. of 31 GHz Rx.), **VRF23_NS** (Noise source temp. of 23 GHz Rx.), **AIR_TEMP** (External ambient temp.), **PRESS** (Atmospheric barometric pressure).

Once the data file is generated, it can be provided to the original executable code to calculate the PWV or use additional Python code to calculate the opacity. Figure 7 shows some results from the radiometer subsystems: A) shows the voltage transitions for each receiver switch, indicating pin switches transitioning from 5V (ON) to 0V (OFF), the 31 GHz noise source's switch control transitioning from -10V (ON) to 0.75V (OFF) and 23 GHz noise source's switch transitioning

from -10V (ON) to 2.75V (OFF); B) shows the acquisition and signal processing of temperature modules at the RF cases, monitoring the temperature change during the controller's process. After 5:30 hours the temperatures clearly show the PID curve of the process, with the visibly clean data curves due to the median filter applied from software.

The weather station was tested outside the laboratory to see the performance of the temperature and humidity sensor (HTU21) and the barometric pressure/altitude sensor (BMP280); see sample data in Figure 8.

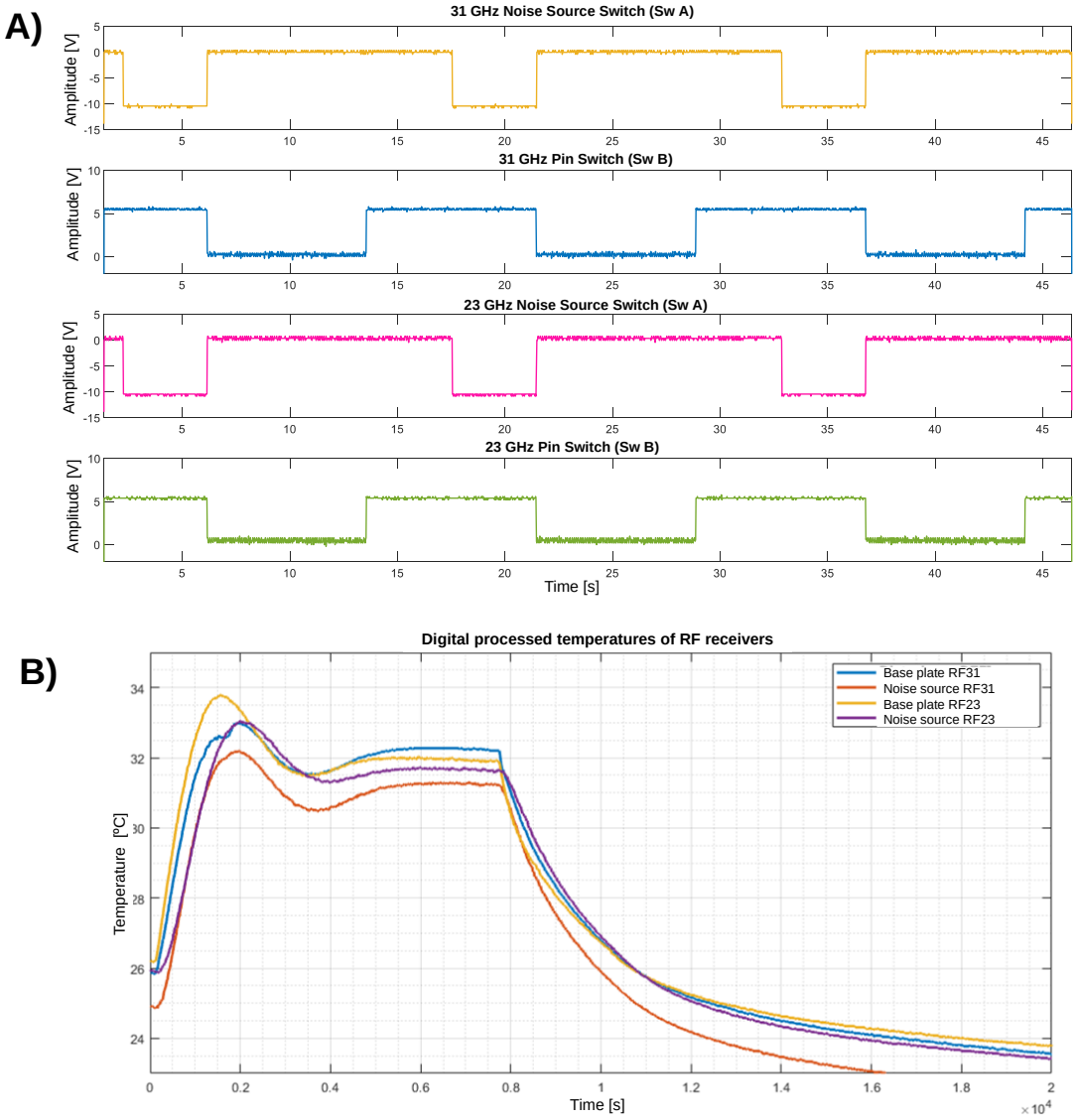

Figure 7. A) RF switching time signals. B) RF receivers' temperature sensors behavior during controller performance.

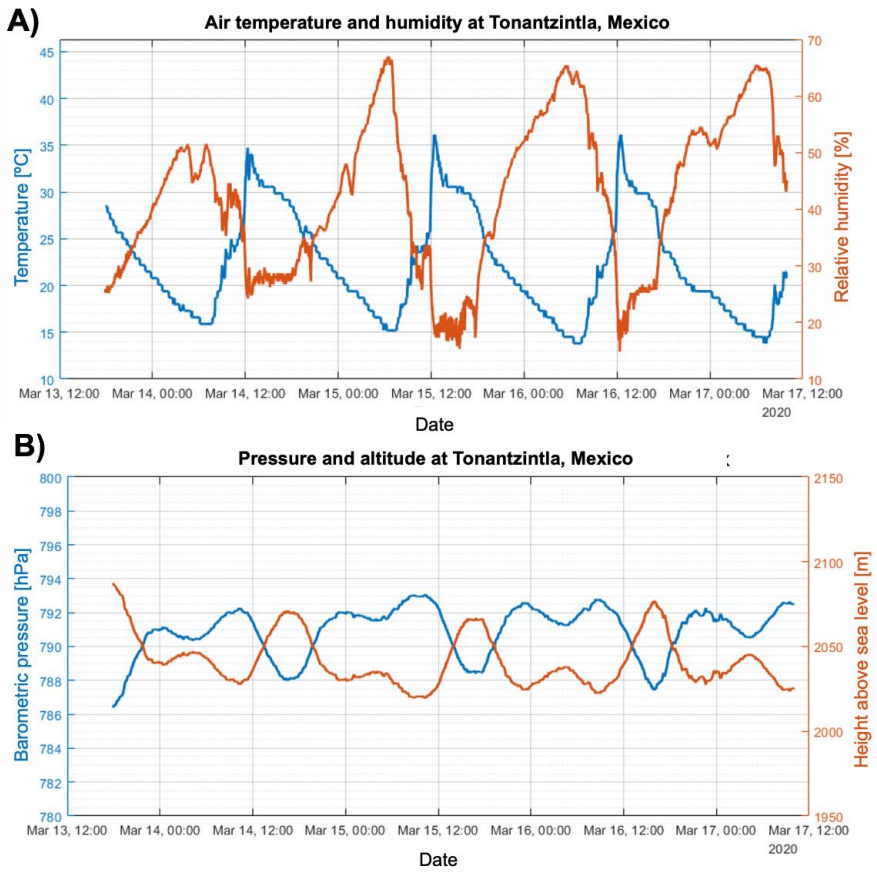

Figure 8. Graphs of A) temperature/humidity and B) barometric pressure/altitude sensors from the radiometer´s weather station.

Figure 9, shows the results from the data acquisition of the three thermal sources of the 23 and 31 GHz channels. As can be seen from the plots, the DC voltage levels are clearly shown for every RF channel. These values are saved for calculation of opacity or PWV according to file structure described in previous paragraphs. At time of writing, due to limitations imposed on activities outside of the lab and the logistics involved, no sky measurements were taken to date.

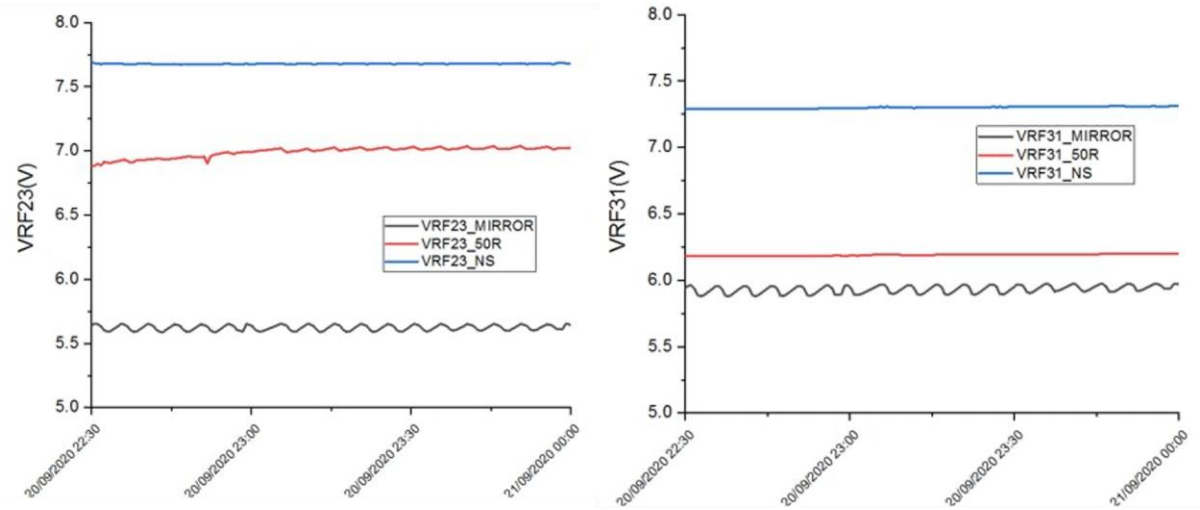

Figure 9. Graphs of 23 and 31 GHz antenna voltages, 50Ω load and Noise source reference voltages.

4. CONCLUSIONS

We have successfully upgraded the control and data acquisition sub-systems of a dual 23.8/31.5 GHz channel radiometer for measurements of water vapor for site characterization. The core of the system is integrated by the low-cost single board computer *Raspberry Pi 3B+*. The new system provides a configurable ADC and thermometry for the RF components to regulate its operating temperature. A meteorological station was also implemented to provide real time measurements of ambient temperature, relative humidity and barometric pressure. The WVR-III core design allows for elevation and azimuth control with the motor control provided by a PWM interface and an H-bridge which are also controlled by the RPi-3B+. New capabilities have been added to the radiometer to allow Ethernet, Wi-Fi, 4G-LTE and USB communication to send the data to the cloud and access the data remotely.

The instrument has been extensively tested in laboratory conditions observing different ambient loads and testing the internal cold and hot source references, Figure 10 shows the instrument new assembly in laboratory. Once COVID-19 travel restrictions have been eased, the instrument will be deployed to *Sierra Negra* the site of the *Large Millimeter Telescope*, the *Hartebeesthoek Radio Astronomy Observatory* and *Gamsberg* in Namibia to measure the atmosphere of known and new radio astronomical sites.

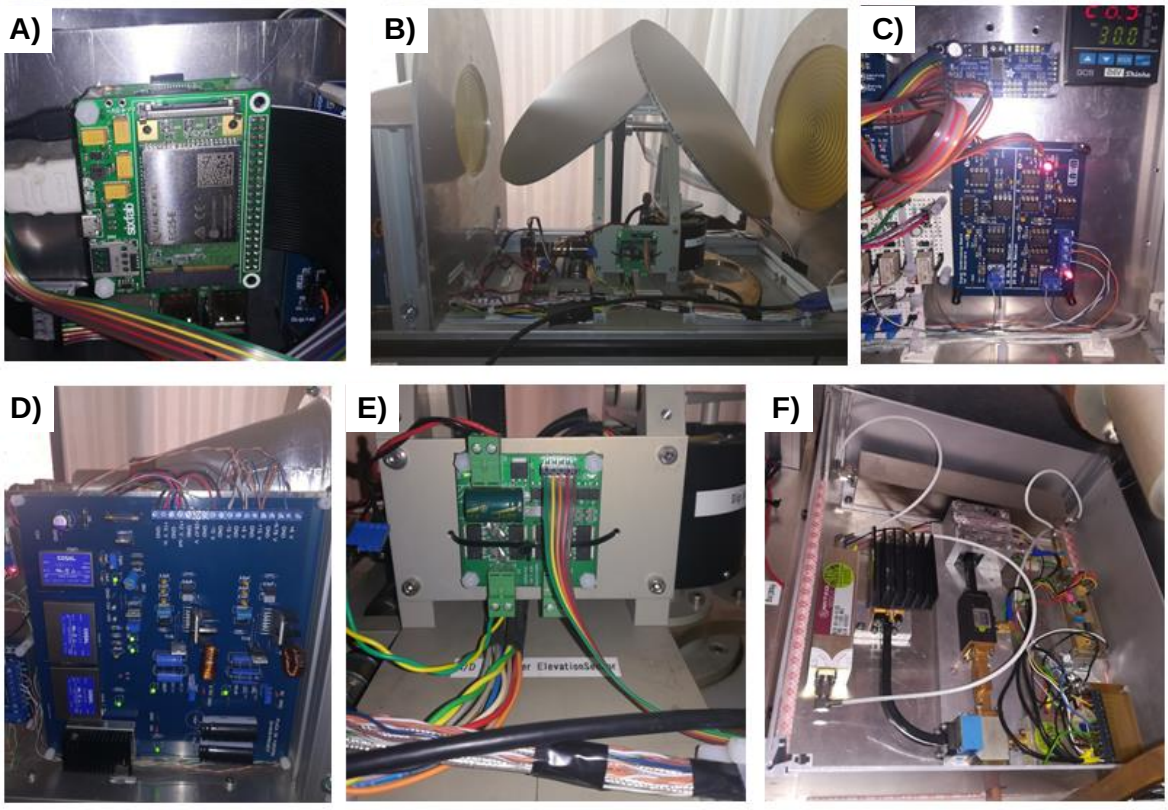

Figure 10. Upgraded WVR-III at INAOE's laboratory. A) *Raspberry Pi 3B+*with *SixFab* 3G/4G base shield HAT; B) 23 and 31 GHz mirrors and entrance to horns, and general view of motors drives and control; C) Center: signal conditioning board; top: PCA9685 serial PWM interface; right: temperature controller; D) Power supply module; E) DFRobot AQMH2407 dual H bridge to drive-up the servo; F) Internal view of the 31 GHz RF box.

5. ACKNOWLEDGMENTS

We acknowledge the *Consejo Nacional de Ciencia y Tecnología* (CONACyT-Mexico), the *National Research Foundation* (South Africa), the *Universidad Nacional Autónoma de México* (UNAM) for the funds provided to develop this project, and the *Hartebeesthoek Radio Astronomy Observatory* and the *University of Pretoria* for providing the instrument.

REFERENCES

[1] Pinilla-Ruíz C., "Interacción de la Radiación con la Atmósfera," Universidad de Jaén, España (2014).
[2] Pravilov A. M. "Radiometry in Modern Scientific Experiments," Springer, USA (2011).
[3] Condon J. J., Ramson S. M., "Radiometer," National Radio Astronomy Observatory, https://www.cv.nrao.edu/course/astr534/Radiometers.html, USA (2016).
[4] Botha R., "Manager of Geodesy Programme of Hartebeesthoek Radio Astronomy Observatory," South African Radio Astronomy Observatory, Personal Contact: roelf@hartrao.ac.za South Africa (2020).
[5] CAPTECH GmbH, "WVR III (Microwave- Water-Vapor-Radiometer) Technical Documentation," ETH Institute for Geodesy and Photogrammetry, Switzerland (2000).
[6] Radiometer Physics GmbH, "RPG-Tip-225 Technical Instrument Manual," Radiometer Physics GmbH, Germany (2013).
[7] Hiriart D., "Survey Radiometer Owner's Manual and Radiometer Utilities," University of Massachusetts Amherst, USA (1994).
[8] Numpy Project, "NumPy Documentation," https://numpy.org/ (2020).
[9] The MathWorks Inc., "Curve Fitting Toolbox," MATLAB Documentation, https://www.mathworks.com/help/curvefit/, USA (2019).
[10] The MathWorks Inc., "System Identification Toolbox," MATLAB Documentation, https://la.mathworks.com/help/ident/, USA (2019).
[11] The MathWorks Inc., "PID Tuner," Simulink Documentation, https://la.mathworks.com/help/control/ref/pidtuner-app.html, USA (2019).
[12] Stander, T., et al., "Progress toward improved water vapour radiometry: An overview of the South Africa-Mexico Bilateral Programme", Proc. SPIE 11445 (2020 (accepted)).
[13] Bearnes B. and DiCola T., and Bill E., "Adafruit Explore & Learn ADS1115," Adafruit Industries, https://learn.adafruit.com/adafruit-4-channel-adc-breakouts/downloads, USA (2019).
[14] Rembor K. and DiCola T., "Adafruit Explore & Learn LSM9DS1," Adafruit Industries, https://learn.adafruit.com/adafruit-lsm9ds1-accelerometer-plus-gyro-plus-magnetometer-9-dof-breakout/overview, USA (2019).
[15] Bearnes B. and Rembor K., "Adafruit Explore & Learn HTU-21D," Adafruit Industries, https://learn.adafruit.com/adafruit-htu21d-f-temperature-humidity-sensor/python-circuitpython, USA (2018).
[16] Bearnes B. and DiCola T., "Adafruit Explore & Learn BMP280," Adafruit Industries, https://learn.adafruit.com/adafruit-bmp280-barometric-pressure-plus-temperature-sensor-breakout/downloads, USA (2019).
[17] Mountain Z. and Wang F., "EC25 Mini PCIe Hardware Design LTE Module Series," Quectel Wireless Solutions, https://www.codico.com/shop/media/datasheets/Quectel_EC25_Mini_PCIe_Hardware_Design_V1.0.pdf, China (2016).
[18] SixFab Inc., "Introduction to Raspberry Pi 3g-4g/Lte Base Shield," SixFab Documentation, https://docs.sixfab.com/docs/raspberry-pi-3g-4g-lte-base-shield-introduction ,Germany (2019).